Available online at www.sciencedirect.com

SciVerse ScienceDirect

journal homepage: www.elsevier.com/locate/jmbbm

Research paper

Characterization of the anisotropic mechanical properties of excised human skin

Aisling Ní Annaidh[a,b,c,*], *Karine Bruyère*[d], *Michel Destrade*[a,e], *Michael D. Gilchrist*[a,f], *Mélanie Otténio*[d]

[a] *School of Mechanical & Materials Engineering, University College Dublin, Belfield, Dublin 4, Ireland*
[b] *UPMC Univ Paris 06, UMR 7190, Institut Jean Le Rond D'Alembert, F-75005 Paris, France*
[c] *CNRS, UMR 7190, Institut Jean Le Rond D'Alembert, F-75005 Paris, France*
[d] *Université de Lyon, F-69622, Lyon, IFSTTAR, LBMC, UMR_T9406, F-69675, Bron, Université Lyon 1, Villeurbanne, France*
[e] *School of Mathematics, Statistics and Applied Mathematics, National University of Ireland Galway, Galway, Ireland*
[f] *School of Human Kinetics, University of Ottawa, Ontario K1N 6N5, Canada*

ARTICLE INFO

Article history:
Received 19 April 2011
Received in revised form
17 August 2011
Accepted 19 August 2011
Published online 31 August 2011

Keywords:
Soft tissue
Langer lines
Tensile properties
Histology

ABSTRACT

The mechanical properties of skin are important for a number of applications including surgery, dermatology, impact biomechanics and forensic science. In this study, we have investigated the influence of location and orientation on the deformation characteristics of 56 samples of excised human skin. Uniaxial tensile tests were carried out at a strain rate of 0.012 s^{-1} on skin from the back. Digital Image Correlation was used for 2D strain measurement and a histological examination of the dermis was also performed. The mean ultimate tensile strength (UTS) was 21.6 ± 8.4 MPa, the mean failure strain 54% ± 17%, the mean initial slope 1.18 ± 0.88 MPa, the mean elastic modulus 83.3 ± 34.9 MPa and the mean strain energy was 3.6 ± 1.6 MJ/m^3. A multivariate analysis of variance has shown that these mechanical properties of skin are dependent upon the orientation of the Langer lines ($P < 0.0001 - P = 0.046$). The location of specimens on the back was also found to have a significant effect on the UTS ($P = 0.0002$), the elastic modulus ($P = 0.001$) and the strain energy ($P = 0.0052$). The histological investigation concluded that there is a definite correlation between the orientation of the Langer lines and the preferred orientation of collagen fibres in the dermis ($P < 0.001$). The data obtained in this study will provide essential information for those wishing to model the skin using a structural constitutive model.

© 2011 Elsevier Ltd. All rights reserved.

1. Introduction

Skin is a complex multi-layered material which can be broadly divided into three main layers, the epidermis, the dermis, and the hypodermis. The epidermis consists of cells and cellular debris, the dermis consists of mostly networks of the fibrous proteins collagen, reticulin and elastin (Wilkes et al., 1973), and the hypodermis is primarily made up of

* *Corresponding author at:* School of Mechanical & Materials Engineering, University College Dublin, Belfield, Dublin 4, Ireland. Tel.: +353 1 716 1991.
E-mail address: aisling.niannaidh@ucd.ie (A. Ní Annaidh).

1751-6161/$ - see front matter © 2011 Elsevier Ltd. All rights reserved.
doi:10.1016/j.jmbbm.2011.08.016

LifeNet Exhibit 2031
Embody, et al. v. LifeNet, IPR2025-00249
Page 1

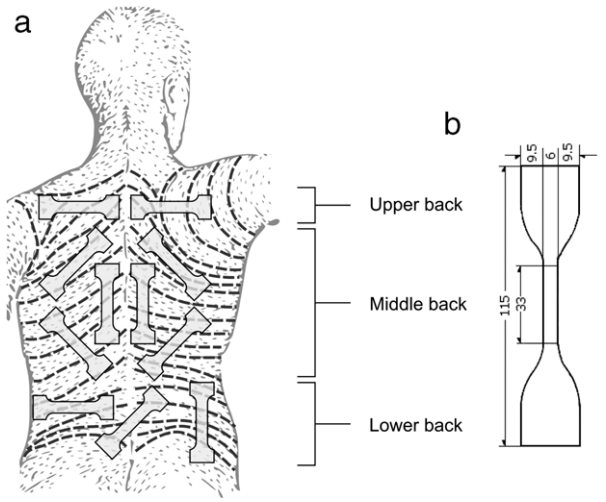


Fig. 1 – (a) Orientation of samples from the back. Specimens are superimposed onto a map of the Langer lines to indicate their orientation with respect to the lines (Langer, 1861). (b) Dimensions of custom made dye (mm).

connective tissue and fat lobules. Collagen fibres account for 75% of the dry weight of dermal tissue (Wilkes et al., 1973) and it is these fibres which are responsible for the strength of the skin.

Skin is a highly non-linear, anisotropic, viscoelastic and nearly incompressible material. A typical stress–stretch graph for skin exhibits non-linear behaviour and its response is usually described as three-phase (Brown, 1973). In the initial loading phase, skin is very compliant and large deformation occurs at a relatively low applied load. At this stage, the fibres are largely unaligned. In the second phase, the stiffness of the skin gradually increases as the fibres align themselves in the direction of the load applied. The third phase is an almost linear phase whereby the stiffness increases rapidly as the collagen fibres are mostly aligned and the overall mechanical response becomes dependent on the mechanical properties of the collagen fibres, which are stiffer than elastin by three grades of magnitude.

That skin is anisotropic was recognized as far back as the 19th century by Langer (1861), who mapped the natural lines of tension which occur within the skin. These lines are identified by puncturing the skin with a circular device. The wounds then assume an elliptical shape and by joining the major axes of the ellipses, a system of lines can be drawn as shown in Fig. 1(a). These lines are known as the Langer lines. While the Langer lines are the best known skin tension lines, many variations on the original lines proposed by Langer have been made. These include the Cox lines (Cox, 1941), Kraissl lines (Kraissl, 1951) and (RSTL) relaxed skin tension lines (Borges, 1984).

Early tensile tests suggested that the deformation characteristics of skin are dependent upon specimen orientation with respect to the Langer lines (Ridge and Wright, 1966). More recent work conducted using optical coherence elastography in-vivo, indicates a large difference between the Young moduli of skin along directions parallel and orthogonal to the Langer lines (Liang and Boppart, 2010).

In this study, we provide new experimental data of in-vitro human skin focusing, in particular, on the anisotropic properties of the skin. We also quantify the degree of anisotropy of the mechanical properties with respect to their Langer line orientation. Finally, we perform a quantitative histological analysis on the dermis of the test samples to examine a possible correlation between the orientation of the Langer lines and the preferred direction of collagen fibres.

While many recent publications on skin report in-vivo experiments (Delalleau et al., 2008; Flynn et al., 2011; Moerman et al., 2009), here we have limited our experiments to in-vitro uniaxial tensile tests. As discussed by Holzapfel, there are a number of issues involved with tensile tests (Holzapfel, 2006): The structural integrity of the samples may be disturbed at the lateral edges and due to the soft nature of the test material, it is difficult to insert samples without subjecting them to an axial load. Despite these shortcomings, it was decided to perform in-vitro tensile tests over in-vivo testing for a number of reasons. First, in-vitro tests provide simple stress–strain relationships that can be modelled and quantified easily, since their boundary conditions are well defined. Second, for the application of this work in a further study into the dynamic rupture of skin, we are also interested in failure and rupture of skin, and in-vitro testing makes it possible to test until failure.

Most in-vitro investigations use human skin substitutes such as pigskin, silicone or polyurethane (McCarthy et al., 2007; Gilchrist et al., 2008; Jor et al., 2011; McCarthy et al., 2010) and in-vitro tests on human skin are particularly rare. Those classical publications which do use human skin often rely on outdated equipment and their results can be difficult to interpret (Cox, 1941; Jansen and Rottier, 1958b). However, the development of accurate constitutive models depends heavily upon their material definitions. This study aims to provide new material data for human skin which can be applied to constitutive models in a number of technical areas such as razor blade manufacture, cosmetics, surgical simulation, forensic pathology and impact biomechanics. Uniaxial tensile tests alone are not sufficient to determine multi-dimensional material models for soft tissues and using a simple non-linear regression analysis to determine constitutive parameters may result in non-unique solutions, ill-conditioned equations and slow convergence rates. Ideally, testing of skin would involve planar biaxial tests with an in-plane shear, and separate through-thickness shear tests. While advanced testing protocols like these are not yet available, simple tension tests remain important because they serve to evaluate the level of anisotropy and to provide data which can later be used as validation for models constructed using more complicated testing methods (Holzapfel and Ogden, 2009). Moreover, model parameters can be provided directly from a histological study of the collagen fibre alignment in the dermis which allows for reasonable determination of material responses (Holzapfel, 2006).

2. Materials and method

2.1. *Specimen preparation*

Tensile tests and preparation were carried out in IFSTTAR (Institut français des sciences et technologies des transports,

LifeNet Exhibit 2031
Embody, et al. v. LifeNet, IPR2025-00249
Page 2

Table 1 – Information on each test subject.

Gender	Age (years)	Time elapsed[a]	Label
Male	97	9	A
Male	91	3	B
Female	97	2	C
Female	81	3	D
Male	89	3	E
Female	85	4	F
Female	86	4	G

[a]Number of days elapsed after death prior to testing.

de l'aménagement et des réseaux), France. French law allows human corpses that have been donated to science to be used for research purposes. The ethics committee within IFSTTAR approved the use of human biological material. Skin was excised from seven subjects: three males and four females. The average age of the subjects was 89 ± 6 years and none had any related skin diseases. Table 1 provides details on the gender and age of each subject at the time of death along with the number of days that elapsed prior to testing.

Only the skin from the back of the subject was available for use. This was excised from the body with a scalpel. Each sample of skin was cut into a dogbone shape specimen, according to the ASTM D412 standard tensile test method for vulcanized rubber, using a custom made dye (see Fig. 1). Each specimen then had the epidermis and any underlying adipose tissue carefully removed with a scalpel. The thickness of the skin after removal of adipose tissue was measured using a Vernier Callipers and the mean thickness was 2.56 ± 0.39 mm. It was observed that skin removed from the lumbar area of the back contained more adipose tissue than skin from other areas of the back. The dimensions of the test specimens were measured before and after excision. Specimens were obtained in various orientations, shown in Fig. 1, to correlate the specimens with the direction of the Langer lines. Each sample was grouped into one of three categories: parallel, perpendicular, or at 45° to the Langer lines. The skin was stored in moistened paper and refrigerated at 4 °C until it was ready to be tested. A total of 56 samples were tested successfully. Although it is widely accepted that preconditioning is necessary at small and intermediate strains, at higher strains the stress–strain response is not significantly affected by preconditioning (Eshel and Lanir, 2001). The samples were therefore not pre-conditioned prior to testing.

2.2. *Tensile tests*

Tensile tests were performed using a universal tensile test machine. Samples were clamped using specially designed anti-slip clamps, to counteract the tendency of samples to slip in ordinary grips. The velocity of the cross-head was 50 mm/min. The tensile load was measured with a 1 kN piezoelectric load cell. Each tensile test was videoed with two Dalsa Falcon 1.4M100 digital video cameras at 20 frames/second. This was to record any abnormal behaviour during the experiments and also for the subsequent use of digital image correlation. The gauge length and width were both measured optically. For these tests, the strain rate was 0.012 s^{-1}, nominally the same strain rate as in tests carried out by Jansen and Rottier (1958a).

The main focus of this study is an investigation into the hyperelastic properties of skin and how these vary according to orientation and location. We thus considered the tensile tests to be taking place at quasi-static speed, and ignored viscoelastic effects for the purpose of constitutive hyperelastic modelling (for examples of studies where this route is chosen, see Jor et al., 2011, Pailler-Mattei et al., 2008, Evans and Holt, 2009 or Cavicchi et al., 2009). Further creep and stress relaxation tests, requiring additional skin samples, would need to be carried out to characterize the viscoelasticity of skin.

2.3. *Digital Image Correlation*

The stretch ratio was calculated via the displacement cell attached to the cross-head of the tensile machine. As validation, the stretch ratio was also calculated via Digital Image Correlation (DIC). DIC is a full-field optical strain measurement technique which uses image registration to measure the 2D or 3D deformation of a material. The technique works by tracking unique features on the surface of the material as it deforms. The correlations were based on images taken with the two Dalsa Falcon video cameras and processed using Vic2D software (Version 2009—Correlated Solution, Inc.). Black spray paint was applied to the surface of the skin to create the desired random speckled pattern necessary for the correlation.

2.4. *Histology*

Three biopsies were procured from the test specimens prior to testing. These biopsies were placed in a formaldehyde solution for fixation for a period exceeding 48 h. Biopsies were then embedded in paraffin prior to slicing. Each biopsy was sectioned at 5 μm intervals, creating a number of thin slices which were transferred onto glass slides. Biopsies were sliced in three orthogonal planes as shown in Fig. 2. The samples were then stained using a Van Gieson stain, which differentiates collagen fibres by making them appear pink/red. Images were taken from each slide using a Nikon E80i transmission microscope and CCD camera. The orientation of collagen fibres were then calculated in a fully-automated customized MATLAB routine using the Image Processing Toolbox. The algorithm is described further in Ní Annaidh et al. (submitted for publication).

2.5. *Statistical analysis*

A statistical analysis of the experimental results was carried out using the general linear model procedure implemented in SAS 9.1 (SAS Institute Inc., USA). A multivariate analysis of variance was utilized, followed by the Tukey–Kramer post-hoc test, to determine the influence of orientation and location of the various test samples. Significance levels for these tests were set to $P < 0.05$. When performing this test a normal distribution was assumed. To ensure our data set followed a normal distribution, a Lilliefors test was performed using the *lillietest* function in MATLAB R2007b.

LifeNet Exhibit 2031
Embody, et al. v. LifeNet, IPR2025-00249
Page 3

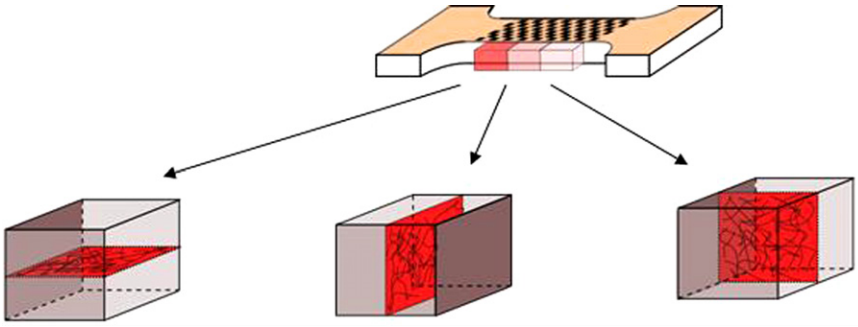


Fig. 2 – Biopsies of skin samples for the purpose of histological staining. Note that the biopsies have been sliced in three orthogonal planes.

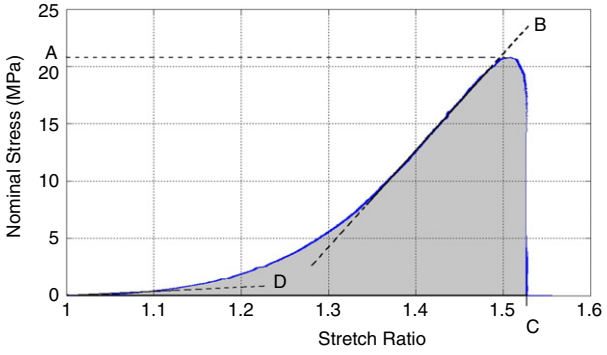


Fig. 3 – Typical stress–stretch graph for the experiments. The ultimate tensile strength is the maximum stress until failure of the specimen and is indicated by A. The elastic modulus is defined as the slope of the linear portion of the curve shown by B. The failure stretch is the maximum stretch obtained before failure and is shown by C. The initial slope is the slope of the curve at infinitesimal strains and is shown by D. The strain energy is the energy per unit volume consumed by the material during the experiment and is represented by the area under the curve.

3. Results

For each tensile test performed, a force–displacement curve was obtained. The nominal stress was then calculated by dividing the force by the undeformed cross sectional area of the specimen. The stretch ratio was calculated by dividing the current length of the specimen by the initial length. In this way, nominal stress vs. stretch ratio graphs were plotted for each specimen. A number of characteristics from these curves were identified as descriptive parameters. They are illustrated in Fig. 3.

3.1. *Intra-subject and inter-subject variations*

A difficulty often encountered with the testing of biological tissue is the large variation in experimental results across samples. Fig. 4(a) indicates the intra-subject and inter-subject variations in the UTS between samples. There is a large intra-subject variation for each subject which is primarily due to anisotropy. Fig. 4(b) shows the stress–stretch graphs of ten different samples taken from five subjects. Note that the left and right samples were adjacent to one another but also in the same orientation with respect to the Langer lines. The similarity of these responses between the left and right samples from the same subjects indicates good repeatability of our experiments.

3.2. *Deformation of specimens after excision*

It is known that both shrinkage and expansion of specimens can occur upon excision from the body (Cox, 1941; Jansen and Rottier, 1958a; Ridge and Wright, 1966; Lanir and Fung, 1974). This is due to the release of residual stresses within the skin. What remains unclear is the level of residual stress present within the skin and how this may vary with the orientation of specimens. It has been suggested that the shrinkage of excised specimens is greatest in the direction of the Langer lines (Ridge and Wright, 1966); however our results did not corroborate this. Our results showed that 73% of all samples expanded upon excision, while only 27% of all samples shrunk. Of the samples that expanded, there was a mean expansion of 5.1 ± 3.4%. Amongst the samples that shrunk, a mean shrinkage of 3 ± 2.9% was recorded. This is far below the reported maximum figure of 20% shrinkage for human skin (Jansen and Rottier, 1958a) and 40% shrinkage provided for pig skin (Jor et al., 2011).

3.3. *Histology*

The collagen fibres were assumed to form an interweaving lattice structure, as first postulated by Ridge and Wright (1966). Here, the preferred orientation is defined as the mean of the orientations of two families of interweaving fibres. It was assumed that the collagen fibres are distributed according to a transversely isotropic and π-periodic von Mises distribution. The von Mises distribution is commonly assumed for directional data. The standard π-periodic von Mises distribution is normalized and the resulting distribution is given as follows.

$$\rho(\Theta) = 4\sqrt{\frac{b}{2\pi}}\frac{\exp[b(\cos(2\Theta)+1)]}{\operatorname{erfi}\sqrt{2b}} \tag{1}$$

where Θ is the mean orientation of fibres and b is the concentration parameter associated with the von Mises distribution. The parameter b was evaluated by the

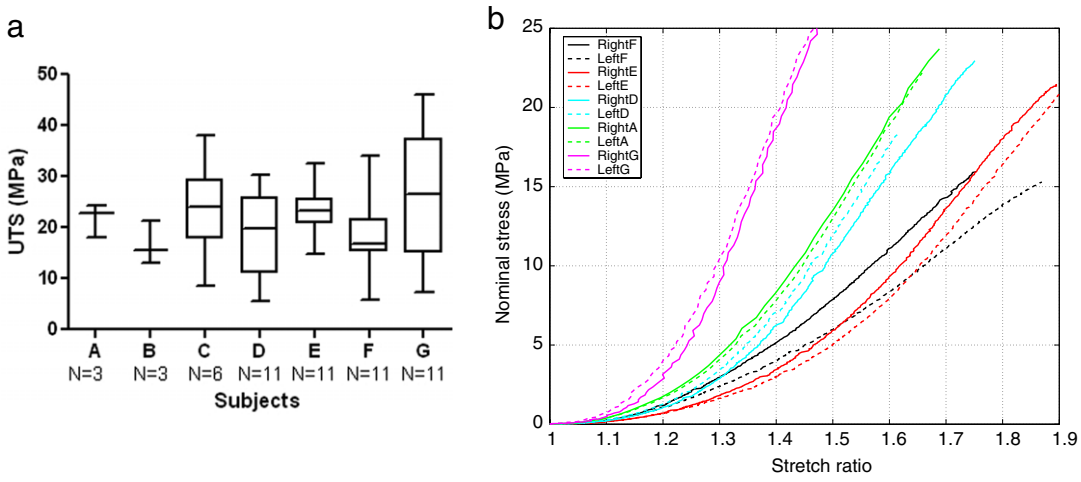


Fig. 4 – (a) Box and whisker plot of the intra-subject and inter-subject variations in UTS ($N = 56$) for subjects A–G. The whiskers indicate the max and min. The boxes represent the lower and the upper quartile and the line is the median. (b) Stress–stretch response of adjacent samples from the upper back (see Fig. 1) with the same orientation ($N = 10$). Colours indicate different subjects while solid and dashed lines indicate samples to the right and left of the spinal line respectively. This illustrates the inter-subject and intra-subject variations between adjacent samples with the same orientation.

Table 2 – Mean orientation of collagen fibres and their Langer Line orientations. (Note that the data given is axial data i.e. it represents undirected lines and does not distinguish between θ and $\pi + \theta$ (Jones, 2006) e.g. the orientation of 0° and 180° are equivalent.)

Orientation with respect to Langer lines	Preferred orientation, Θ	Level of dispersion, b
0°	40°	0.5222
0°	16°	1.1605
0°	16°	1.1471
0°	168°	0.6004
45°	40°	0.8388
45°	61°	0.7926
45°	46°	0.7453
45°	53°	0.4209
45°	57°	0.8326
45°	83°	0.9330
90°	73°	0.9007
90°	120°	0.6197

approximation given by Fisher (1993) using the CircStat package available on the MATLAB file exchange (Berens, 2009).

Table 2 shows the calculated concentration parameter b, the mean orientation of collagen fibres and the orientation with respect to the Langer lines. A Pearson correlation test was carried out to test for a correlation between the preferred orientation obtained through histology and the perceived orientation of the Langer lines. The correlation was deemed to be significant ($P < 0.001$) with a Pearson R value of 0.9487 and an R^2 value of 0.9000.

3.4. *Influence of orientation*

Specimens were analysed by considering their orientation with respect to the Langer lines (parallel, perpendicular or at 45° to the Langer lines, see Fig. 1). A multiway analysis of variance found the orientation of the Langer lines to have a significant effect on the UTS ($P < 0.0001$), the strain energy ($P = 0.0101$), the elastic modulus ($P = 0.0002$), the initial slope ($P = 0.0375$), and the failure stretch ($P = 0.046$). The interaction between orientation and location was also tested i.e., whether the effect of orientation was dependent upon location. This interaction between orientation and location was found to be significant only for the failure stretch ($P = 0.0118$). The presence of this interaction is probably due to small differences in the perceived orientation of the Langer lines over the body. Fig. 5 and Table 3 display the variations in the mechanical properties between samples of different orientations. The variations are substantial, except for the failure stretch, where the effect of the orientation is complicated by the existence of the interaction between orientation and location.

3.5. *Influence of location*

When results were grouped into three locations (upper back, middle back and lower back, see Fig. 1), a multiway analysis of variance also found the location of specimens to have a significant effect on the UTS ($P = 0.0002$), the strain energy ($P = 0.0052$) and the elastic modulus ($P = 0.001$), but neither on the failure stretch nor the initial slope. Fig. 6 displays variations in the mechanical properties between different locations on the back for the three properties which showed a significant effect i.e., the elastic modulus, UTS and strain energy. Note that there was no significant effect noted for either the initial slope or the failure stretch.

3.6. *Digital image correlation*

An important feature of DIC is its ability to calculate local strains throughout the plane of the test specimens. Fig. 7(a) shows a comparison between the local stretch values, obtained through DIC, and the overall stretch values, obtained

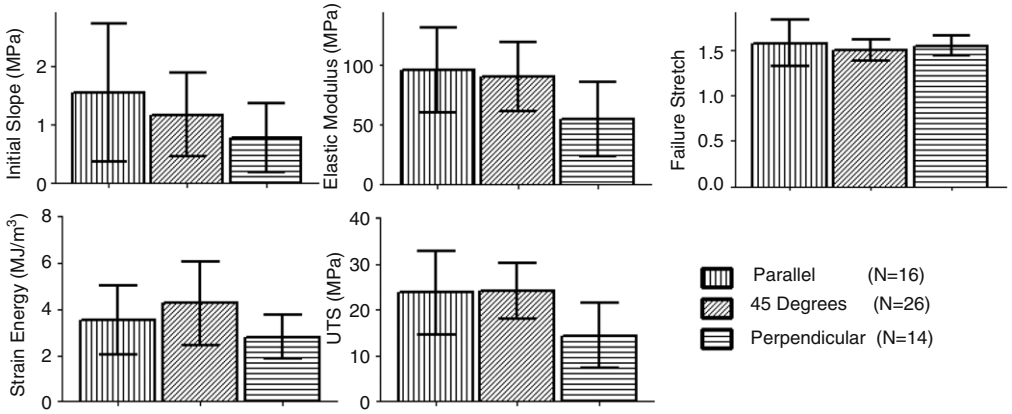


Fig. 5 – Influence of orientation on the initial slope, elastic modulus, failure stretch, strain energy and UTS. Values given include mean and standard deviations.

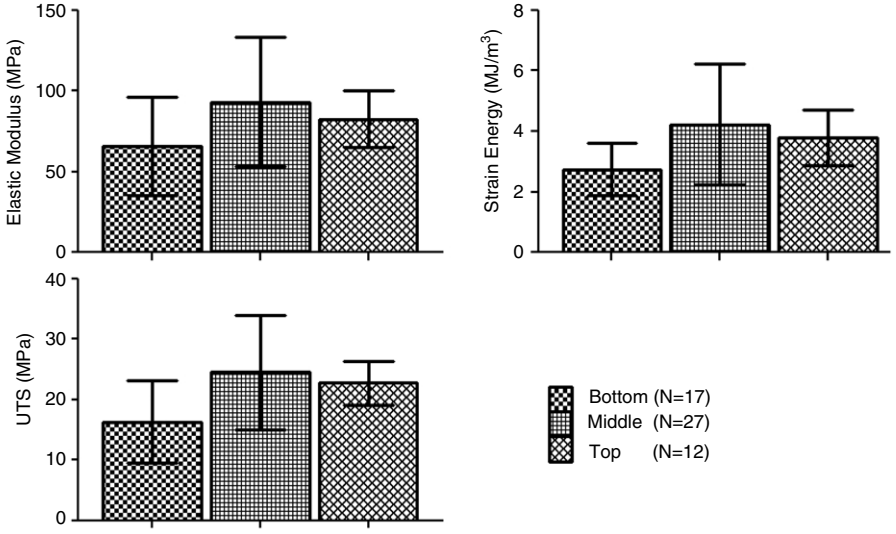


Fig. 6 – Influence of location on the back for the elastic modulus, strain energy and UTS. Values given include mean and standard deviations.

from the displacement sensor (DS), throughout the duration of a test. It can be seen that there is good agreement for most of the duration of the test. However, upon closer inspection, it was found that a local magnification of the stretch ratio occurred just before rupture, close to the rupture site (for magnitudes, see Table 4). Fig. 7(b) shows the distribution of strains throughout the sample for a frame just before rupture. For some samples this magnification was very localized while for others it was distributed over a larger area. A similar result was reported by Jacquemoud et al. (2007) who found that at the rupture site, the local strain values can be up to twice as large as what is measured using overall specimen strains calculated over the entire length of a specimen.

4. Discussion

When comparing our own data to that in the literature, it can be seen that there is much variation between authors. This is to be expected for biological tissues. First, because of the biological variability between subjects; second, because of the anisotropic nature of skin itself; and third, because of the sensitivity of biological tissues to test conditions. In the absence of extensive published literature on the properties of in vitro human skin from the back, Table 5 compares results obtained from the literature from a range of locations and test methods to our own results. The mean ultimate tensile strength was 21.6 ± 8.4 MPa, the mean failure strain 54 ± 17%, the mean initial slope 1.18 ± 0.88 MPa, the mean elastic modulus 83.3 ± 34.9 MPa and the mean strain energy was 3.6 ± 1.6 MJ/m^3. It can be seen that our experimental results fall within the ranges found in the literature for in-vitro tests. However there is a large variation with the various types of in-vivo tests. The reasons for this difference has been widely discussed and the primary causes are due to the properties of skin changing once removed from the body; the different testing methods employed; and an inability to establish boundary conditions and to isolate the skin's behaviour from its surrounding tissue in vivo. Furthermore, the modulus defined in-vivo is in the low-strain range,

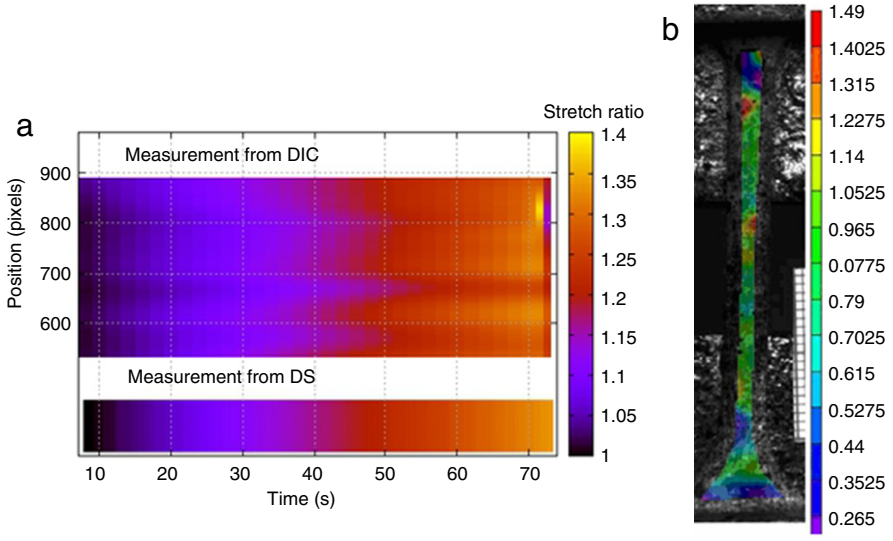


Fig. 7 – (a) Comparison of stretch measurement from DIC and DS over the length of the specimen throughout the duration of a given tensile test. (b) Distribution of local Lagrangian strains just before rupture. Note the area of localized magnification in red. This is the location where rupture subsequently occurred.

Table 3 – Mean ± standard deviation for each orientation/location group.

Langer line orientation	Location	N	UTS (MPa)	Strain energy (MJ/m^3)	Failure stretch	Elastic modulus (MPa)	Initial slope (MPa)
Parallel	Middle	9	28.64 ± 9.03	4.28 ± 1.49	1.46 ± 0.07	112.47 ± 36.49	1.21 ± 0.97
Parallel	Bottom	7	17.60 ± 4.77	2.54 ± 0.76	1.74 ± 0.32	73.81 ± 19.41	1.95 ± 1.34
45°	Top	12	22.7 ± 3.61	3.80 ± 0.92	1.52 ± 0.10	82.62 ± 17.36	0.99 ± 0.51
45°	Middle	9	28.85 ± 7.87	5.38 ± 2.59	1.52 ± 0.15	103.49 ± 41.20	1.33 ± 0.96
45°	Bottom	5	20.23 ± 4.18	3.31 ± 0.67	1.43 ± 0.04	82.81 ± 18.43	1.30 ± 0.60
Perpendicular	Middle	9	16.53 ± 5.71	2.98 ± 0.89	1.52 ± 0.08	63.75 ± 24.59	0.91 ± 0.68
Perpendicular	Bottom	5	10.56 ± 8.41	2.44 ± 1.04	1.61 ± 0.14	37.66 ± 36.41	0.54 ± 0.33

Table 4 – Local and overall maximum stretch ratios for five different samples. Local magnification of the stretch ratio occurs just before rupture.

Sample	Local max stretch ratio	Overall specimen stretch ratio
1	1.47	1.38
2	1.45	1.40
3	1.65	1.45
4	1.70	1.48
5	1.70	1.50

whereas the modulus calculated here is in the high-strain range. The in-vivo modulus should then be compared with the initial slope, rather than with the elastic modulus.

It has been well documented over the years that the deformation characteristics of skin are dependent upon specimen orientation, but few authors describe the level of anisotropy involved in much detail. In this study, we have provided statistical information on the effect of the Langer line orientation on the UTS, strain energy, failure strain, initial slope, and elastic modulus. We have been unable to establish a link between the level of shrinkage of skin upon excision and the orientation of the Langer lines. Instead, we found that the majority of samples actually expanded upon excision. The reason for this discrepancy may be two-fold; first, the skin has been excised from the back, not the abdomen, which may be more extensible to accommodate the shrinkage and expansion of the stomach. Second, the skin samples were excised from elderly subjects which naturally exhibit less extensibility. This has been previously noted by Jansen and Rottier (1958a,b) who stated that skin excised from elderly subjects was more likely to expand rather than retract, when compared to younger subjects. Finally, the authors noted that while shrinkage of the skin may have occurred directly after excision from the body, after subcutaneous fat was removed, the samples often expanded. This poses the question on the effect the subcutaneous fat has on the level of shrinkage/expansion of the skin, usually thought to be solely due to the release of residual stresses in the skin.

Previous studies show that the properties of skin are dependent upon specimen location (Haut, 1989; Sugihara et al., 1991). Our results also indicate that the UTS, strain energy and elastic modulus vary depending on the location. However, as only skin from the back was available for testing, the location of specimens could only be categorized into upper back, middle back and lower back regions. It was nonetheless advantageous to gain information on skin from the back because it is seldom as readily available as that from the abdominal area.

Table 5 – Comparison of results obtained to results in the literature. All experiments were carried out in-vitro on excised human skin. Results are displayed as means (± standard deviation) and ranges.

Author	Test type	UTS (MPa)	Failure strain (%)	Elastic modulus (MPa)	Initial slope (MPa)	Site[a]	Age
Jansen and Rottier (1958b)	In vitro tension	1–24	17–207	2.9–54.0	0.69–3.7	Ab	0–99
Dunn (1983)	In vitro tension	2–15		18.8	0.1	AB & T	47–86
Vogel (1987)	In vitro tension	5–32	30–115	15–150		V	0–90
Jacquemoud et al. (2007)	In vitro tension	5.7–12.6	27–59	19.5–87.1		F & A	62–98
Agache et al. (1980)	In vivo torsion			0.42–0.85		Back	3–89
Diridollou et al. (1998)	In vivo suction			0.12–0.25		A & F	20–30
Khatyr et al. (2004)	In vivo tension			0.13–0.66		Tibia	22–68
Pailler-Mattei et al. (2008)	In vivo indentation			0.0045–0.008		A	30
Zahouani et al. (2009)	In vivo indentation and static friction			0.0062–0.0021		A	55–70
Our results	In vitro tensile	21.6 ± 8.4	54 ± 17	83.3 ± 34.9	1.18 ± 0.88	Back	81–97

[a]Ab = abdomen, T = thorax, V = various, F = forehead, A = arm.

All subjects were between the ages of 81 and 97. This meant that no comparisons based on the age of subjects could be performed. Numerous other studies have investigated the influence of age on the structure and mechanical behaviour of skin (Vogel, 1987; Haut, 1989; Sugihara et al., 1991). It has been established that progressive straightening of elastin fibres occurs over time (Lavker et al., 1987). This may cause the shortened phase I region of the stress–strain curve leading to an overall reduction in extensibility. The slope of the phase III portion of the curve, however remains relatively constant (Wilkes et al., 1973). Nonetheless, it must be highlighted that the results of this study may not reflect the behaviour of younger skin and consideration must be taken to allow for age-related effects when interpreting these results.

A number of days had elapsed between the time of death and testing (see Table 1), but it has been previously demonstrated that skin samples can be refrigerated for up to 48 h under the right conditions with no discernible effects on the mechanical properties (Daly, 1982) and for up to 21 days for thoracic aortas under certain conditions (Adham et al., 1996).

DIC is a common strain measurement technique in biomechanics, however until now it has been used mostly for in-vivo experiments or at low strains (Moerman et al., 2009). The results yielded from the present use of DIC may be useful in the future as validation for a finite element approach. Also the local maximum strain values reported are of interest to those who wish to model the failure of biological tissues.

In this paper, our data has been examined with respect to the perceived orientation of the Langer lines. However, the Langer lines are known to vary with location, age and gender and no universal pattern of maximum tensions exist (Brown, 1973). The orientation of the Langer lines cannot be identified with certainty unless the skin of a whole cadaver is punctured, an option which was not feasible for this study. Given the importance of the Langer lines on the mechanical properties of the skin, there is a need for patient-specific maps to be established in-vivo and in real time. These could be produced by relying on sophisticated imaging techniques such as those produced by ultrasonic surface wave propagation or optical coherence tomography and may eventually have applications in cosmetic surgery.

Cox (1941) and Stark (1977) both illustrated that the orientations of the Langer lines remain even after the skin is removed from the body and the skin tension released, and concluded that the lines have an anatomical basis. However it remains unclear in the literature whether the Langer lines have a structural basis, and to the authors' knowledge there is no quantitative data published on this point. By identifying the orientation of collagen fibres in the dermis, we have shown that there is a correlation between their orientation and that of the Langer lines. However, it is only when a quantitative study is performed that this becomes apparent.

Knowledge of the collagen fibre orientation along with the stress–strain data presented will also facilitate the determination of material parameters for structurally based constitutive models for skin. While the test method described here is not sufficient to fully describe the full 3D response of the material, Holzapfel (2006) has shown how a combination of tensile tests and histological data can be used to reasonably determine the material parameters of a 3D hyperelastic model. In a companion paper (Ní Annaidh et al., submitted for publication), we use a similar approach in order to determine the material and structural parameters of a suitable anisotropic model, the so-called Gasser–Ogden–Holzapfel model (Gasser et al., 2006), readily implemented into the commercial finite element code, ABAQUS.

Acknowledgements

This research was supported by a Marie Curie Intra European Fellowship within the 7th European Community Framework Programme, awarded to MD. It was also supported by IRCSET (Irish Research Council for Science, Engineering and Technology) through the Ulysses Award, and IRCSET and the Office of the State Pathologist (Irish Department of Justice

LifeNet Exhibit 2031
Embody, et al. v. LifeNet, IPR2025-00249
Page 8

and Law Reform) through the EMBARK scholarship awarded to ANíA. This work was supported by grants from the Ile-de-France Region.

REFERENCES

Adham, M., Gournier, J.-P., Favre, J.-P., De La Roche, E., Ducerf, C., Baulieux, J., Barral, X., Pouyet, M., 1996. Mechanical characteristics of fresh and frozen human descending thoracic aorta. Journal of Surgical Research 64 (1), 32–34.

Agache, P., Monneur, C., Leveque, J., De Rigal, J., 1980. Mechanical properties and young's modulus of human skin in vivo. Archives of Dermatological Research 269, 221–232.

Berens, P., 2009. Circstat: a MATLAB toolbox for circular statistics. Journal of Statistical Software 31 (10).

Borges, A., 1984. Relaxed skin tension lines (RSTL) versus other skin lines. Plastic Reconstructive Surgery 73 (1), 144–150.

Brown, I.A., 1973. A scanning electron microscope study of the effects of uniaxial tension on human skin. British Journal of Dermatology 89, 383–393.

Cavicchi, A., Gambarotta, L., Massab, R., 2009. Computational modeling of reconstructive surgery: the effects of the natural tension on skin wrinkling. Finite Elements in Analysis and Design 45 (8–9), 519–529.

Cox, H., 1941. The cleavage lines of the skin. British Journal of Surgery 29 (114), 234–240.

Daly, C.H., 1982. Biomechanical properties of dermis. Journal of Investigative Dermatology 79, 17–20.

Delalleau, A., Josse, G., Lagarde, J.M., Zahouani, H., Bergheau, J.M., 2008. Characterization of the mechanical properties of skin by inverse analysis combined with an extensometry test. Wear 264 (5–6), 405–410.

Diridollou, S., Berson, M., Vabre, V., Black, D., Karlsson, B., Auriol, F., Gregoire, J.M., Yvon, C., Vaillant, L., Gall, Y., Patat, F., 1998. An in vivo method for measuring the mechanical properties of the skin using ultrasound. Ultrasound in Medicine & Biology 24 (2), 215–224.

Dunn, M.G., Silver, F.H., 1983. Viscoelastic behavior of human connective tissues: Relative contribution of viscous and elastic components. Connective Tissue Research 12 (1), 59–70.

Eshel, H., Lanir, Y., 2001. Effects of strain level and proteoglycan depletion on preconditioning and viscoelastic responses of rat dorsal skin. Annals of Biomedical Engineering 29 (2), 164–172.

Evans, S.L., Holt, C.A., 2009. Measuring the mechanical properties of human skin in vivo using digital image correlation and finite element modelling. The Journal of Strain Analysis for Engineering Design 44 (5), 337–345.

Fisher, N., 1993. Statistical Analysis of Circular Data. Cambridge University Press, Cambridge.

Flynn, C., Taberner, A., Nielsen, P., 2011. Mechanical characterisation of in vivo human skin using a 3D force-sensitive microrobot and finite element analysis. Biomechanics and Modeling in Mechanobiology 10, 27–38.

Gasser, T., Ogden, R.W., Holzapfel, G., 2006. Hyperelastic modelling of arterial layers with distributed collagen fibre orientations. Journal of the Royal Society Interface 3, 15–35.

Gilchrist, M.D., Keenan, S., Curtis, M., Cassidy, M., Byrne, G., Destrade, M., 2008. Measuring knife stab penetration into skin simulant using a novel biaxial tension device. Forensic Science International 177 (1), 52–65.

Haut, R.C., 1989. The effects of orientation and location on the strength of dorsal rat skin in high and low speed tensile failure experiments. Journal of Biomechanical Engineering 111 (2), 136–140.

Holzapfel, G.A., 2006. Determination of material models for arterial walls from uniaxial extension tests and histological structure. Journal of Theoretical Biology 238 (2), 290–302.

Holzapfel, G.A., Ogden, R.W., 2009. On planar biaxial tests for anisotropic nonlinearly elastic solids. A continuum mechanical framework. Mathematics and Mechanics of Solids 14 (5), 474–489.

Jacquemoud, C., Bruyere-Garnier, K., Coret, M., 2007. Methodology to determine failure characteristics of planar soft tissues using a dynamic tensile test. Journal of Biomechanics 40 (2), 468–475.

Jansen, L., Rottier, P., 1958a. Comparison of the mechanical properties of strips of human abdominal skin excised from below and from above the umbilic. Dermatologica 117, 252–258.

Jansen, L., Rottier, P., 1958b. Some mechanical properties of human abdominal skin measured on excised strips. Dermatologica 117, 65–83.

Jones, T.A., 2006. Matlab functions to analyze directional (azimuthal) data—I: single-sample inference. Computers & Geosciences 32 (2), 166–175.

Jor, J.W.Y., Nielsen, P.M.F., Nash, M.P., Hunter, P.J., 2011. Modelling collagen fibre orientation in porcine skin based upon confocal laser scanning microscopy. Skin Research and Technology.

Khatyr, F., Imberdis, C., Vescovo, P., Varchon, D., Lagarde, J.M., 2004. Model of the viscoelastic behaviour of skin in vivo and study of anisotropy. Skin research and technology 10, 96–103.

Kraissl, C., 1951. The selection of appropriate lines for elective surgical incisions. Plastic and Reconstructive Surgery 8 (1), 1–28.

Langer, K., 1861. On the anatomy and physiology of the skin. The Imperial Academy of Science, Vienna. British Journal of Plastic Surgery 17 (31), 93–106. Reprinted in (1978).

Lanir, Y., Fung, Y.C., 1974. Two-dimensional mechanical properties of rabbit skin–II. Experimental results. Journal of Biomechanics 7 (2), 171–174.

Lavker, R., Zheng, P., Dong, G., 1987. Aged skin: a study by light, transmission electron, and scanning electron microscopy. Journal of Investigative Dermatology 88, 419–428.

Liang, X., Boppart, S.A., 2010. Biomechanical properties of in vivo human skin from dynamic optical coherence elastography. IEEE Transactions on Biomedical Engineering 57 (4), 953–959.

McCarthy, C.T., Hussey, M., Gilchrist, M.D., 2007. On the sharpness of straight edge blades in cutting soft solids: part I—indentation experiments. Engineering Fracture Mechanics 74 (14), 2205–2224.

McCarthy, C.T., Ní Annaidh, A., Gilchrist, M.D., 2010. On the sharpness of straight edge blades in cutting soft solids: part II—analysis of blade geometry. Engineering Fracture Mechanics 77 (3), 437–451.

Moerman, K.M., Holt, C.A., Evans, S.L., Simms, C.K., 2009. Digital image correlation and finite element modelling as a method to determine mechanical properties of human soft tissue in vivo. Journal of Biomechanics 42 (8), 1150–1153.

Ní Annaidh, A., Bruyère, K., Destrade, M., Gilchrist, M., Maurini, C., Otténio, M., Saccomandi, G., 2011. Automated estimation of collagen fibre dispersion in the dermis and its contribution to the anisotropic behaviour of skin (submitted for publication).

Pailler-Mattei, C., Bec, S., Zahouani, H., 2008. In vivo measurements of the elastic mechanical properties of human skin by indentation tests. Medical Engineering & Physics 30 (5), 599–606. doi:10.1016/j.medengphy.2007.06.011.

Ridge, M., Wright, V., 1966. The directional effects of skin. A bioengineering study of skin with particular reference to Langer's lines. Journal of Investigative Dermatology 46 (4), 341–346.

LifeNet Exhibit 2031
Embody, et al. v. LifeNet, IPR2025-00249
Page 9

Stark, H.L., 1977. Directional variations in the extensibility of human skin. British Journal of Plastic Surgery 30 (2), 105–114.

Sugihara, T., Ohura, T., Homma, K., Igawa, H., 1991. The extensibility in human skin: variation according to age and site. British Journal of Plastic Surgery 44, 418–422.

Vogel, H., 1987. Age dependence of mechanical and biochemical properties of human skin. Bioengineering and the Skin 3, 67–91.

Wilkes, G., Brown, I., Wildnauer, R., 1973. The biomechanical properties of skin. CRC Critical Reviews in Bioengineering 1 (4), 453–495.

Zahouani, H., Pailler-Mattei, C., Sohm, B., Vargiolu, R., Cenizo, V., Debret, R., 2009. Characterization of the mechanical properties of a dermal equivalent compared with human skin in vivo by indentation and static friction tests. Skin Research and Technology 15 (1), 68–76.

LifeNet Exhibit 2031
Embody, et al. v. LifeNet, IPR2025-00249
Page 10